COMPDYN 2015
5th ECCOMAS Thematic Conference on
Computational Methods in Structural Dynamics and Earthquake Engineering
M. Papadrakakis, V. Papadopoulos, V. Plevris (eds.)
Crete Island, Greece, 25–27 May 2015

# WAVE BASED DESIGN OPTIMISATION OF COMPOSITE STRUCTURES OPERATING IN DYNAMIC ENVIRONMENTS

**D. Chronopoulos[1], M. Collet[2], M. Ichchou[3], and I. Antoniadis[4]**

[1]Division of Materials, Mechanics and Structures
University Park, The University of Nottingham, NG7 2RD, UK
e-mail: dimitrios.chronopoulos@nottingham.ac.uk

[2]LTDS, UMR-CNRS 5513
36 Avenue Guy de Collongue, 69130 Ecully, France
e-mail: manuel.collet@ec-lyon.fr

[3]Ecole Centrale de Lyon
36 Avenue Guy de Collongue, 69130 Ecully, France
e-mail: mohamed.ichchou@ec-lyon.fr

[4] Machine Design and Control Systems Section
School of Mechanical Engineering, National Technical University of Athens, Greece
e-mail: antogian@central.ntua.gr

**Keywords:** Structural design optimisation, Vibroacoustic response, Composite structures, Wave propagation

**Abstract.** *The optimal mechanical and geometric characteristics for layered composite structures subject to vibroacoustic excitations are derived. A Finite Element description coupled to Periodic Structure Theory is employed for the considered layered panel. Structures of arbitrary anisotropy as well as geometric complexity can thus be modelled by the presented approach. Initially, a numerical continuum-discrete approach for computing the sensitivity of the acoustic wave characteristics propagating within the modelled periodic composite structure is exhibited. The first and second order sensitivities of the acoustic transmission coefficient expressed within a Statistical Energy Analysis context are subsequently derived as a function of the computed acoustic wave characteristics. Having formulated the gradient vector as well as the Hessian matrix, the optimal mechanical and geometric characteristics satisfying the considered mass, stiffness and vibroacoustic performance criteria are sought by employing Newton's optimisation method.*

## 1 INTRODUCTION

Layered and complex structures are nowadays widely used within the aerospace, automotive, construction and energy sectors with a general increase tendency, mainly because of their high stiffness-to-mass ratio and the fact that their mechanical characteristics can be designed to suit the particular purposes. Unluckily however, this high stiffness-to-mass ratio being responsible for the increased mechanical efficiency, at the same time induces high acoustic transmission through the structure. The need for simultaneously optimising an industrial structure of minimum mass and maximum static stiffness, while attaining satisfactory dynamic response performance levels is a challenging task for the modern engineer; especially when considering acoustic transmission through a layered structure which depends on the mechanical and geometric characteristics of each individual layer, resulting in a great number of design parameters to be optimised.

The numerical analysis of wave propagation within periodic structures was firstly considered in [1], while the work was extended to two dimensional media in [2, 3]. The so called Wave Finite Element (WFE) method was introduced in [4, 5] in order to facilitate the post-processing of the eigenproblem solutions and further improve the computational efficiency of the method. The interest in predicting the vibroacoustic response of a structure in a wave context is far from being new with the pioneering works of the authors in [6, 7, 8, 9] being probably the earliest ones. A layer-wise model for the prediction of acoustic wave propagation within continuous layered structures was presented in [10]. More recently, the prediction of the acoustic wave characteristics based on FE formulations allowed for more complex structures to be included in the dynamic response computations [11, 12, 13, 14, 15, 16, 17].

Structural sensitivity analysis is of great importance for understanding the overall impact of a design parameter variation to the structural performance which is to be optimised. Accurate sensitivity models are an important tool for design optimization, system identification as well as for statistical mechanics analysis. Many authors [18, 19, 20, 21] have been focusing on the eigenvalue derivative analysis of a structural system. With regard to the variability analysis of the waves travelling within a structural medium the conducted work has been mainly focused on deriving expressions [22, 23] of the stochastic wave parameters from analytical models. In [24] the authors conduct a design sensitivity analysis by a wave based approach. Considering numerical approaches the authors in [25] used Bloch's theorem in conjunction with the FE method in order to calculate the sensitivity of the acoustic waves within an auxetic honeycomb, while with regard to the computation of the variability of the propagating waves the authors in [26, 27] have presented a stochastic WFE method approach for computing the stochastic wave propagation in one dimensional media. With regard to optimising the design characteristics of a layered structure the developed approaches have generally focused on genetic algorithms or particle swarm type techniques [28, 29, 30]. When it comes to optimising the structural design vis-a-vis the dynamic response performance of a structure, wave based optimisation techniques have been developed [31, 32, 33, 34] by adopting Periodic Structure Theory (PST) assumptions.

In this work an established wave based SEA approach is employed in order to predict the vibroacoustic performance of a composite layered panel. The novelty of the work focuses on the derivation of the first and second order sensitivity of the acoustic transmission coefficient expressed through SEA with respect to the structural design characteristics of the modelled structure. The considered design parameters include the entirety of the mechanical characteristics, the density as well as the thickness of each individual structural layer. Non conservative structural systems are also modelled by the exhibited approach. Employing a three dimensional

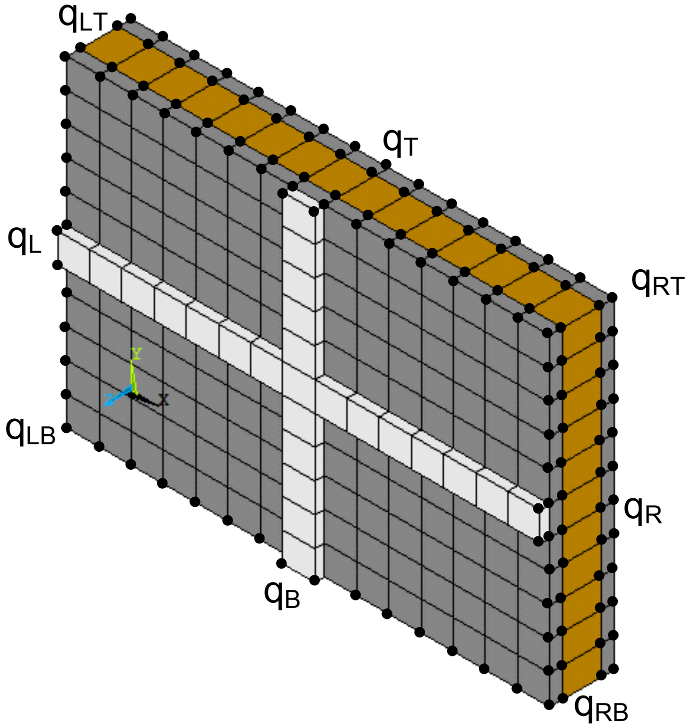


Figure 1: Caption of a FE modelled composite layered panel

FE description of the modelled structure allows for capturing the entirety of the sound transmitting propagating structural waves, while employing a PST formulation allows for drastically reducing the computational cost related to calculating the SEA parameters and the Hessian matrix for each configuration. Although not discussed in this work, the method is straightforward to apply to curved structures by expressing the FE structural matrices and wave propagation properties in polar coordinates.

## 2 ACOUSTIC WAVE SENSITIVITY

### 2.1 Formulation of the PST for an arbitrary structural segment

A periodic segment of a panel having arbitrary layering is hereby considered (see Fig.1) with $L_x$, $L_y$ its dimensions in the $x$ and $y$ directions respectively. The segment is modelled using a conventional FE software. The mass, damping and stiffness matrices of the segment $\mathbb{M}$, $\mathbb{C}$ and $\mathbb{K}$ are extracted and the DoF set $\mathbf{q}$ is reordered according to a predefined sequence such as:

$$\mathbf{q} = \{\mathbf{q_I} \;\; \mathbf{q_B} \;\; \mathbf{q_T} \;\; \mathbf{q_L} \;\; \mathbf{q_R} \;\; \mathbf{q_{LB}} \;\; \mathbf{q_{RB}} \;\; \mathbf{q_{LT}} \;\; \mathbf{q_{RT}}\}^\top \tag{1}$$

corresponding to the internal, the interface edge and the interface corner DoF (see Fig.1). The free harmonic vibration equation of motion for the modelled segment is written as:

$$[\mathbb{K} + \mathrm{i}\omega\mathbb{C} - \omega^{\mathbf{2}}\mathbb{M}]\mathbf{q} = \mathbf{0} \tag{2}$$

The analysis then follows as in [3] with the following relations being assumed for the displacement DoF under the passage of a time-harmonic wave:

$$\begin{aligned} \mathbf{q_R} &= \mathrm{e}^{-i\varepsilon_x}\mathbf{q_L}, \quad \mathbf{q_T} = \mathrm{e}^{-i\varepsilon_y}\mathbf{q_B} \\ \mathbf{q_{RB}} &= \mathrm{e}^{-i\varepsilon_x}\mathbf{q_{LB}}, \quad \mathbf{q_{LT}} = \mathrm{e}^{-i\varepsilon_y}\mathbf{q_{LB}}, \quad \mathbf{q_{RT}} = \mathrm{e}^{-i\varepsilon_x - i\varepsilon_y}\mathbf{q_{LB}} \end{aligned} \tag{3}$$

with $\varepsilon_x$ and $\varepsilon_y$ the propagation constants in the $x$ and $y$ directions related to the phase difference between the sets of DoF. The wavenumbers $k_x$, $k_y$ are directly related to the propagation constants through the relation:

$$\varepsilon_x = k_x L_x, \quad \varepsilon_y = k_y L_y \tag{4}$$

Considering Eq.3 in tensorial form gives:

$$\mathbf{q} = \begin{bmatrix} \mathbf{I} & \mathbf{0} & \mathbf{0} & \mathbf{0} \\ \mathbf{0} & \mathbf{I} & \mathbf{0} & \mathbf{0} \\ \mathbf{0} & \mathbf{I}\mathrm{e}^{-i\varepsilon_y} & \mathbf{0} & \mathbf{0} \\ \mathbf{0} & \mathbf{0} & \mathbf{I} & \mathbf{0} \\ \mathbf{0} & \mathbf{0} & \mathbf{I}\mathrm{e}^{-i\varepsilon_x} & \mathbf{0} \\ \mathbf{0} & \mathbf{0} & \mathbf{0} & \mathbf{I} \\ \mathbf{0} & \mathbf{0} & \mathbf{0} & \mathbf{I}\mathrm{e}^{-i\varepsilon_x} \\ \mathbf{0} & \mathbf{0} & \mathbf{0} & \mathbf{I}\mathrm{e}^{-i\varepsilon_y} \\ \mathbf{0} & \mathbf{0} & \mathbf{0} & \mathbf{I}\mathrm{e}^{-i\varepsilon_x - i\varepsilon_y} \end{bmatrix} \mathbf{x} = \mathbf{R}\mathbf{x} \tag{5}$$

with $\mathbf{x}$ the reduced set of DoF: $\mathbf{x} = \{\mathbf{q_I} \ \ \mathbf{q_B} \ \ \mathbf{q_L} \ \ \mathbf{q_{LB}}\}^\top$. The equation of free harmonic vibration of the modelled segment can now be written as:

$$[\mathbf{R}^*\mathbb{K}\mathbf{R} + \mathrm{i}\omega\mathbf{R}^*\mathbb{C}\mathbf{R} - \omega^{\mathbf{2}}\mathbf{R}^*\mathbb{M}\mathbf{R}]\mathbf{x} = \mathbf{0} \tag{6}$$

with $^*$ denoting the Hermitian transpose. The most practical procedure for extracting the wave propagation characteristics of the segment from Eq.6 is injecting a set of assumed propagation constants $\varepsilon_x$, $\varepsilon_y$. The set of these constants can be chosen in relation to the direction of propagation towards which the wavenumbers are to be sought and according to the desired resolution of the wavenumber curves. Eq.6 is then transformed into a standard eigenvalue problem and can be solved for the eigenvector $\mathbf{x}$ which describe the deformation of the segment under the passage of each wave type at an angular frequency equal to the square root of the corresponding eigenvalue $\lambda = \omega^2$. It is noted that the computed angular frequency quantities $\omega = \omega_r + \mathrm{i}\omega_i$ will have $\mid \omega_i \mid > 0$ implying complex values for the wavenumbers of the propagating wave types, otherwise interpreted as spatially decaying motion and from which the loss factor of each computed wave type $w$ can directly be determined.

A complete description of each passing wave including its $x$ and $y$ directional wavenumbers and its wave shape for a certain frequency is therefore acquired. It is noted that the periodicity condition is defined modulo $2\pi$, therefore solving Eq.6 with a set of $\varepsilon_x$, $\varepsilon_y$ varying from 0 to $2\pi$ will suffice for capturing the entirety of the structural waves. Further considerations on reducing the computational expense of the problem are discussed in [3]. It should be noted that only propagating waves will be considered in the subsequent analysis.

### 2.2 Parametric sensitivity

For an undamped structural segment the sensitivity of the real eigenvalues $\lambda_p$ can be written as

$$\frac{\partial \lambda_p}{\partial \beta_i} = \mathbf{x}_p^\top \left( \frac{\partial \mathbf{K}}{\partial \beta_i} - \lambda_p \frac{\partial \mathbf{M}}{\partial \beta_i} \right) \mathbf{x}_p \tag{7a}$$

$$\begin{aligned}\frac{\partial^2 \lambda_p}{\partial \beta_j \partial \beta_i} =& \mathbf{x}_p^\top \left( \frac{\partial^2 \mathbf{K}}{\partial \beta_j \partial \beta_i} - \lambda_p \frac{\partial^2 \mathbf{M}}{\partial \beta_j \partial \beta_i} - \frac{\partial \lambda_p}{\partial \beta_j}\frac{\partial \mathbf{M}}{\partial \beta_i} - \frac{\partial \lambda_p}{\partial \beta_i}\frac{\partial \mathbf{M}}{\partial \beta_j} \right) \mathbf{x}_p \\ &+ \mathbf{x}_p^\top \left( \frac{\partial}{\partial \beta_j} \Big[ \mathbf{K} - \lambda_p \mathbf{M} \Big] \right) \frac{\partial \mathbf{x}_p}{\partial \beta_i} + \mathbf{x}_p^\top \left( \frac{\partial}{\partial \beta_i} \Big[ \mathbf{K} - \lambda_p \mathbf{M} \Big] \right) \frac{\partial \mathbf{x}_p}{\partial \beta_j}\end{aligned} \tag{7b}$$

with the sensitivity of the real mode shapes $\frac{\partial \mathbf{x}_p}{\partial \beta_j}$ to be calculated by the approach exhibited in [18]. The global mass and stiffness matrices $\mathbb{M}, \mathbb{K}$ of the structural segment are formed by adding the local mass and stiffness matrices of individual FEs. Eq.7 can be written as

$$\frac{\partial \lambda_p}{\partial \beta_i} = \mathbf{x}_p^\top \left( \mathbf{R}^* \frac{\partial \mathbb{K}}{\partial \beta_i} \mathbf{R} - \lambda_p \mathbf{R}^* \frac{\partial \mathbb{M}}{\partial \beta_i} \mathbf{R} \right) \mathbf{x}_p \tag{8a}$$

$$\begin{aligned}\frac{\partial^2 \lambda_p}{\partial \beta_j \partial \beta_i} =& \mathbf{x}_p^\top \left( \mathbf{R}^* \frac{\partial^2 \mathbb{K}}{\partial \beta_j \partial \beta_i} \mathbf{R} - \lambda_p \mathbf{R}^* \frac{\partial^2 \mathbb{M}}{\partial \beta_j \partial \beta_i} \mathbf{R} - \mathbf{R}^* \frac{\partial \lambda_p}{\partial \beta_j}\frac{\partial \mathbb{M}}{\partial \beta_i} \mathbf{R} - \mathbf{R}^* \frac{\partial \lambda_p}{\partial \beta_i}\frac{\partial \mathbb{M}}{\partial \beta_j} \mathbf{R} \right) \mathbf{x}_p + \\ & \mathbf{x}_p^\top \left( \frac{\partial}{\partial \beta_j} \Big[ \mathbf{R}^* \mathbb{K} \mathbf{R} - \lambda_p \mathbf{R}^* \mathbb{M} \mathbf{R} \Big] \right) \frac{\partial \mathbf{x}_p}{\partial \beta_i} + \mathbf{x}_p^\top \left( \frac{\partial}{\partial \beta_i} \Big[ \mathbf{R}^* \mathbb{K} \mathbf{R} - \lambda_p \mathbf{R}^* \mathbb{M} \mathbf{R} \Big] \right) \frac{\partial \mathbf{x}_p}{\partial \beta_j}\end{aligned} \tag{8b}$$

For the conservative system it is known however that $\frac{\partial \lambda_p}{\partial \beta_i} = \frac{\partial (\omega_p^2)}{\partial \beta_i}$, therefore

$$\frac{\partial \lambda_p}{\partial \beta_i} = \frac{\dfrac{\partial (\omega_p^2)}{\partial \omega_p}}{\dfrac{\partial \beta_i}{\partial \omega_p}} = 2\omega_p \frac{\partial \omega_p}{\partial \beta_i} \Leftrightarrow \frac{\partial \omega_p}{\partial \beta_i} = \frac{1}{2\omega_p}\frac{\partial \lambda_p}{\partial \beta_i} \tag{9a}$$

$$\frac{\partial^2 \lambda_p}{\partial \beta_j \partial \beta_i} = 2\frac{\partial \omega_p}{\partial \beta_j}\frac{\partial \omega_p}{\partial \beta_i} + 2\omega_p \frac{\partial^2 \omega_p}{\partial \beta_j \partial \beta_i} \Leftrightarrow \frac{\partial^2 \omega_p}{\partial \beta_j \partial \beta_i} = \frac{1}{2\omega_p}\left( \frac{\partial^2 \lambda_p}{\partial \beta_j \partial \beta_i} - 2\frac{\partial \omega_p}{\partial \beta_j}\frac{\partial \omega_p}{\partial \beta_i} \right) \tag{9b}$$

with $\omega_p$ the angular frequency at which the set of $\varepsilon_x$, $\varepsilon_y$ is true for the $p$ wave type described by the $\mathbf{x}_p$ deformation. For the wavenumber sensitivity $\frac{\partial k_p}{\partial \beta_i}$ the following is true

$$\frac{\partial k_p}{\partial \beta_i} = -\frac{\partial k_p}{\partial \omega_p}\frac{\partial \omega_p}{\partial \beta_i} = -\frac{1}{c_{g,p}}\frac{\partial \omega_p}{\partial \beta_i} \tag{10a}$$

$$\frac{\partial^2 k_p}{\partial \beta_j \partial \beta_i} = \frac{1}{c_{g,p}^3}\frac{\partial c_{g,p}}{\partial k_p}\frac{\partial \omega_p}{\partial \beta_j}\frac{\partial \omega_p}{\partial \beta_i} - \frac{1}{c_{g,p}}\frac{\partial^2 \omega_p}{\partial \beta_j \partial \beta_i} \tag{10b}$$

with $c_{g,p} = \frac{\partial \omega_p}{\partial k_p}$ the group velocity associated with the wave type $p$ at frequency $\omega_p$ and the quantities $c_{g,p}$, $\frac{\partial c_{g,p}}{\partial \omega_p}$ to be evaluated by the solution of the baseline structural design.

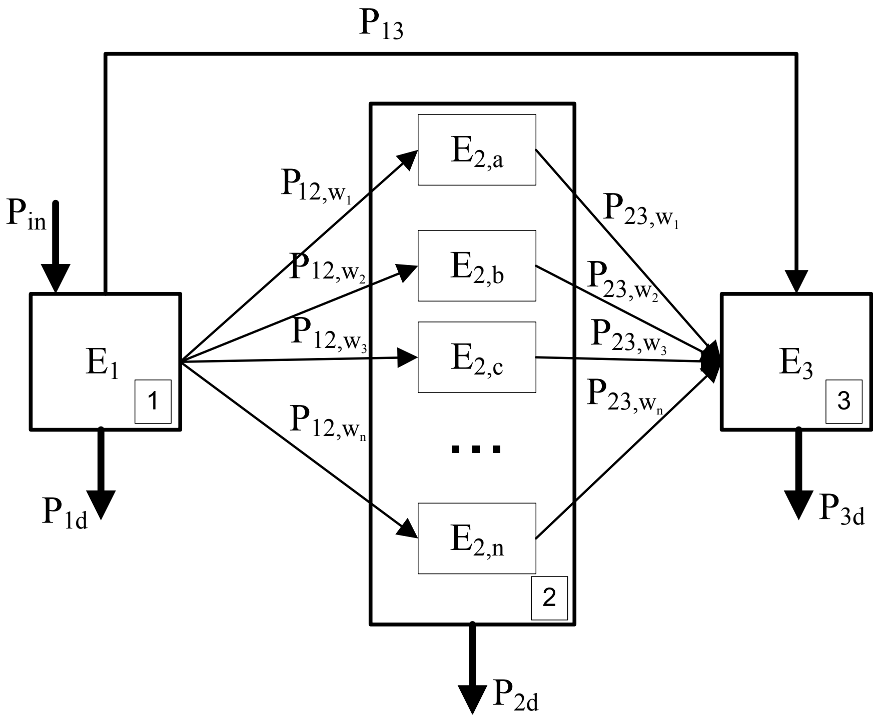


Figure 2: A schematic representation of the SEA power exchanges and energies for the modelled system.

## 3 SEA SENSITIVITY ANALYSIS

### 3.1 The employed SEA model

The impact of the parametric alterations on the vibroacoustic performance of the structure under investigation is exhibited in this section by deriving expressions for the sensitivity of the SEA results with respect to the propagating acoustic waves.

The total acoustic transmission coefficient $\tau$ is one of the most important indices of the vibroacoustic performance of a structure. The system to be modelled comprises one acoustically excited chamber (subsystem 1) and one acoustically receiving chamber (subsystem 3) separated by the modelled composite panel (subsystem 2). It is considered that each wave type is excited and transmits acoustic energy independently from the rest, therefore each considered wave type $w = w_1, w_2 ... w_n$ propagating within the composite panel is considered as a separate SEA subsystem. No flanking transmission is considered in the SEA model. The energy balance between the subsystems as it is considered within an SEA approach (see [8]) is illustrated in Fig.2, in which $E_1, E_3$ stand for the acoustic energy of the source room and the receiving room respectively and $E_2$ for the vibrational energy of the composite panel. Moreover $P_{in}$ is the injected power in the source room, $P_{1d}, P_{2d}$ and $P_{3d}$ stand for the power dissipated by each subsystem and $P_{13}$ is the non-resonant transmitted power between the rooms.

The derivation of an expression for the total acoustic transmission coefficient $\tau$ of the composite structure by merely accounting for its structural dynamic behaviour is exhibited in [11] and reads

$$\tau = \sum_{w=w_1}^{w_n} \tau_w + \frac{P_{13}}{P_{inc}} \tag{11}$$

with $\tau_w$ being the transmission coefficient of the wave type $w$ given as

$$\tau_w = \frac{8\rho^2 c^4 \pi \sigma_{rad,w}^2 n_w}{\rho_s \omega^2 A(\rho_s \omega \eta_w + 2\rho c \sigma_{rad,w})} \tag{12}$$

The non resonant transmission coefficient $\tau_{nr} = P_{13}/P_{inc}$ for a diffused acoustic field can be written as in [10]:

$$\tau_{nr}(\omega) = \frac{1}{\pi(\cos^2\theta_{min} - \cos^2\theta_{max})} \int_0^{2\pi} \int_0^{\theta_{max}} \frac{4Z_0^2}{\mid \mathrm{i}\omega\rho_s + 2Z_0 \mid^2} \sigma(\theta, \phi, \omega) \cos^2\theta \sin\theta \mathrm{d}\theta \mathrm{d}\phi \tag{13}$$

in which $\theta$ and $\phi$ are the incidence angle and the direction angle of the acoustic wave respectively and $Z_0 = \rho c / \cos\theta$ is the acoustic impedance of the medium. The term $\theta_{max}$ stands for the maximum incidence angle, accounting for the diffuseness of the incident field. It is hereby considered that $\theta_{max} = \pi/2$ for all the results presented in the current work. The term $\sigma(\theta, \phi, \omega)$ is the corrected radiation efficiency term. It is used in order to account for the finite dimensions of the panel and it is calculated using a spatial windowing correction technique presented in [35].

Eventually the STL of the panel can be expressed as

$$\mathrm{STL} = 10 \log_{10}\left(\frac{1}{\tau}\right) \tag{14}$$

by definition.

### 3.2 Parametric sensitivity of the total acoustic transmission

In order to formulate the expression of the Hessian matrix describing the variation of the vibroacoustic performance of the structure with respect to its design parameters, the second order derivative of $\tau$ with respect to the considered set of parameters should be derived and expressed as

$$\frac{\partial \tau}{\partial \beta_i} = \sum_{w=w_1}^{w_n} \frac{\partial \tau_w}{\partial \beta_i} + \frac{\partial \tau_{nr}}{\partial \beta_i} \tag{15a}$$

$$\frac{\partial^2 \tau}{\partial \beta_j \partial \beta_i} = \sum_{w=w_1}^{w_n} \frac{\partial^2 \tau_w}{\partial \beta_j \partial \beta_i} + \frac{\partial^2 \tau_{nr}}{\partial \beta_j \partial \beta_i} \tag{15b}$$

while the sensitivity of the STL index can directly be expressed with regard to $\tau$ as

$$\frac{\partial (STL)}{\partial \beta_i} = \frac{\mathrm{d}(STL)}{\mathrm{d}\tau} \frac{\partial \tau}{\partial \beta_i} = -\frac{10}{\ln(10)\tau} \frac{\partial \tau}{\partial \beta_i} \tag{16a}$$

$$\begin{aligned} \frac{\partial^2 (STL)}{\partial \beta_j \partial \beta_i} &= \frac{\partial^2 (STL)}{\partial \tau^2} \frac{\partial \tau}{\partial \beta_j} \frac{\partial \tau}{\partial \beta_i} + \frac{\partial (STL)}{\partial \tau} \frac{\partial^2 \tau}{\partial \beta_j \partial \beta_i} \\ &= \frac{10}{\ln(10)\tau^2} \frac{\partial \tau}{\partial \beta_j} \frac{\partial \tau}{\partial \beta_i} - \frac{10}{\ln(10)\tau} \frac{\partial^2 \tau}{\partial \beta_j \partial \beta_i} \end{aligned} \tag{16b}$$

In the following sections the evaluation of Eq.15 is discussed.

### 3.3 Modal density sensitivity

Using Courant's formula [36], the modal density of each wave type $w$ can be written at a propagation angle $\phi$ as a function of the propagating wavenumber and its corresponding group velocity $c_g$:

$$n_w(\omega,\phi) = \frac{Ak_w(\omega,\phi)}{2\pi^2|c_{g,w}(\omega,\phi)|} \tag{17}$$

The angularly averaged modal density of the structure is therefore given as

$$n_w(\omega) = \int_0^\pi n_w(\omega,\phi)\,\mathrm{d}\phi \tag{18}$$

Thanks to the chain differentiation rule the first and second order derivatives of the modal density for each wave type with respect to design variables $\beta_i$, $\beta_j$ can be expressed as

$$\begin{aligned}\frac{\partial n_w(\omega,\phi)}{\partial\beta_i} &= \frac{\partial n_w(\omega,\phi)}{\partial k_w(\omega,\phi)}\frac{\partial k_w(\omega,\phi)}{\partial\beta_i} + \frac{\partial n_w(\omega,\phi)}{\partial c_{g,w}(\omega,\phi)}\frac{\partial c_{g,w}(\omega,\phi)}{\partial\beta_i} \\ &= \frac{A}{2\pi^2|c_{g,w}(\omega,\phi)|}\frac{\partial k_w(\omega,\phi)}{\partial\beta_i} - \frac{Ak_w(\omega,\phi)\,\mathrm{sgn}(c_{g,w}(\omega,\phi))}{2\pi^2|c_{g,w}(\omega,\phi)|^2}\frac{\partial c_{g,w}(\omega,\phi)}{\partial k_w(\omega,\phi)}\frac{\partial k_w(\omega,\phi)}{\partial\beta_i}\end{aligned} \tag{19a}$$

$$\begin{aligned}\frac{\partial^2 n_w(\omega,\phi)}{\partial\beta_j\partial\beta_i} &= \frac{\partial^2 n_w(\omega,\phi)}{\partial k_w(\omega,\phi)^2}\frac{\partial k_w(\omega,\phi)}{\partial\beta_j}\frac{\partial k_w(\omega,\phi)}{\partial\beta_i} + \frac{\partial n_w(\omega,\phi)}{\partial k_w(\omega,\phi)}\frac{\partial^2 k_w(\omega,\phi)}{\partial\beta_j\partial\beta_i} \\ &+ \frac{\partial^2 n_w(\omega,\phi)}{\partial c_{g,w}(\omega,\phi)^2}\frac{\partial c_{g,w}(\omega,\phi)}{\partial\beta_j}\frac{\partial c_{g,w}(\omega,\phi)}{\partial\beta_i} + \frac{\partial n_w(\omega,\phi)}{\partial c_{g,w}(\omega,\phi)}\frac{\partial^2 c_{g,w}(\omega,\phi)}{\partial\beta_j\partial\beta_i} \\ &= \frac{A}{2\pi^2|c_{g,w}(\omega,\phi)|}\frac{\partial^2 k_w(\omega,\phi)}{\partial\beta_j\partial\beta_i} + \frac{Ak_w(\omega,\phi)\,\mathrm{sgn}(c_{g,w}(\omega,\phi))}{\pi^2|c_{g,w}(\omega,\phi)|^3}\left(\frac{\partial c_{g,w}(\omega,\phi)}{\partial k_w(\omega,\phi)}\right)^2\frac{\partial k_w(\omega,\phi)}{\partial\beta_j}\frac{\partial k_w(\omega,\phi)}{\partial\beta_i} \\ &- \frac{Ak_w(\omega,\phi)\,\mathrm{sgn}(c_{g,w}(\omega,\phi))}{2\pi^2|c_{g,w}(\omega,\phi)|^2}\left(\frac{\partial^2 c_{g,w}(\omega,\phi)}{\partial k_w(\omega,\phi)^2}\frac{\partial k_w(\omega,\phi)}{\partial\beta_j}\frac{\partial k_w(\omega,\phi)}{\partial\beta_i} + \frac{\partial c_{g,w}(\omega,\phi)}{\partial k_w(\omega,\phi)}\frac{\partial^2 k_w(\omega,\phi)}{\partial\beta_j\partial\beta_i}\right)\end{aligned} \tag{19b}$$

while for the spatially averaged modal density

$$\frac{\partial n_w(\omega)}{\partial\beta_i} = \int_0^\pi \frac{\partial n_w(\omega,\phi)}{\partial\beta_i}\mathrm{d}\phi \tag{20a}$$

$$\frac{\partial^2 n_w(\omega)}{\partial\beta_j\partial\beta_i} = \int_0^\pi \frac{\partial^2 n_w(\omega,\phi)}{\partial\beta_j\partial\beta_i}\mathrm{d}\phi \tag{20b}$$

suggesting that the modal density sensitivity can be expressed merely by

- The sensitivity of the characteristics of the waves travelling within the considered structure with respect to the structural design (already determined in Sec.2).
- The sensitivity of the modal density with respect to the characteristics of the waves travelling in it.

A similar approach can be followed for computing all the remaining necessary SEA quantities.

### 3.4 Radiation efficiency sensitivity

In order to avoid the computationally inefficient frequency and directional averaging of the modal dependent radiation efficiency sensitivity $\frac{\partial \sigma_{rad,w}(\omega,\phi)}{\partial \beta_i}$, it is practical to employ expressions introducing a direct wavenumber dependence of $\sigma_{rad,w}$ such as the ones exhibited in [6, 9, 3]. For a generic periodic structure including discontinuities the assumption of sinusoidal mode shapes is no longer valid, therefore the radiation efficiency should be calculated directly from the PST derived wave mode shapes. The radiation efficiency expression as derived in [3] can therefore be employed. For continuous structures, mode shapes of sinusoidal form can be assumed in order to avoid any FE discretization errors in the solution. The set of asymptotic formulas given in [9] can be used for computing the averaged wavenumber dependent radiation efficiency of the panel as

$$\sigma_{rad,w} = \frac{1}{\sqrt{1-\mu^2}} \quad \mu < 0.90 \tag{21a}$$

$$\sigma_{rad,w} = \frac{L_x + L_y}{\pi \mu \kappa L_x L_y \sqrt{\mu^2 - 1}} \left( \ln\left(\frac{\mu+1}{\mu-1}\right) + \frac{2\mu}{\mu^2-1} \right) \quad \mu > 1.05 \tag{21b}$$

$$\sigma_{rad,w} = (0.5 - 0.15 \min(L_x, L_y)/\max(L_x, L_y)) \sqrt{k \min(L_x, L_y)} \quad \mu = 1 \tag{21c}$$

with $\mu = \left(\frac{k_x^2 + k_y^2}{\kappa^2}\right)^{1/2}$, where $\kappa = \omega/c$ is the acoustic wavenumber. In the region $0.90 < \mu < 1.05$ a shape preserving Hermite interpolation function is employed assuring the continuity and double differentiability for the entire spectrum of the $\sigma_{rad,w}$ expression. The sensitivity expressions for the radiation efficiency of the panel can therefore be derived as a function of the propagating flexural wavenumbers by Eq.21, while the interpolation function is used for expressing the sensitivity of $\sigma_{rad,w}$ for the remaining spectrum.

### 3.5 Sensitivity of the resonant acoustic transmission

Taking a look at Eq.12 it can be observed that the sensitivity of the resonant acoustic transmission coefficient with respect to the design parameters of the composite structure can be expressed as

$$\frac{\partial \tau_w}{\partial \beta_i} = \frac{\partial \tau_w}{\partial \sigma_{rad,w}} \frac{\partial \sigma_{rad,w}}{\partial \beta_i} + \frac{\partial \tau_w}{\partial n_w} \frac{\partial n_w}{\partial \beta_i} + \frac{\partial \tau_w}{\partial \rho_s} \frac{\partial \rho_s}{\partial \beta_i} \tag{22a}$$

$$\begin{aligned} \frac{\partial^2 \tau_w}{\partial \beta_j \partial \beta_i} = {} & \frac{\partial^2 \tau_w}{\partial \sigma_{rad,w}^2} \frac{\partial \sigma_{rad,w}}{\partial \beta_j} \frac{\partial \sigma_{rad,w}}{\partial \beta_i} + \frac{\partial \tau_w}{\partial \sigma_{rad,w}} \frac{\partial^2 \sigma_{rad,w}}{\partial \beta_j \partial \beta_i} \\ & + \frac{\partial^2 \tau_w}{\partial n_w^2} \frac{\partial n_w}{\partial \beta_j} \frac{\partial n_w}{\partial \beta_i} + \frac{\partial \tau_w}{\partial n_w} \frac{\partial^2 n_w}{\partial \beta_j \partial \beta_i} \\ & + \frac{\partial^2 \tau_w}{\partial \rho_s^2} \frac{\partial \rho_s}{\partial \beta_j} \frac{\partial \rho_s}{\partial \beta_i} + \frac{\partial \tau_w}{\partial \rho_s} \frac{\partial^2 \rho_s}{\partial \beta_j \partial \beta_i} \end{aligned} \tag{22b}$$

with the transmission coefficient related sensitivity terms being expressed as

$$\frac{\partial \tau_w}{\partial \sigma_{rad,w}} = \frac{16\pi c^4 n_w \rho^2 \sigma_{rad,w}}{A\omega^2 \rho_s(\eta_w \omega \rho_s + 2c\rho\sigma_{rad,w})} - \frac{16\pi c^5 n_w \rho^3 \sigma_{rad,w}^2}{A\omega^2 \rho_s(\eta_w \omega \rho_s + 2c\rho\sigma_{rad,w})^2} \tag{23a}$$

$$\frac{\partial^2 \tau_w}{\partial \sigma_{rad,w}^2} = \frac{16\pi c^4 n_w \rho^2}{A\omega^2 \rho_s(\eta_w \omega \rho_s + 2c\rho\sigma_{rad,w})} - \frac{64\pi c^5 n_w \rho^3 \sigma_{rad,w}}{A\omega^2 \rho_s(\eta_w \omega \rho_s + 2c\rho\sigma_{rad,w})^2} + \frac{64\pi c^6 n_w \rho^4 \sigma_{rad,w}^2}{A\omega^2 \rho_s(\eta_w \omega \rho_s + 2c\rho\sigma_{rad,w})^3} \tag{23b}$$

$$\frac{\partial \tau_w}{\partial n_w} = \frac{8\pi c^4 \rho^2 \sigma_{rad,w}^2}{A\omega^2 \rho_s(\eta_w \omega \rho_s + 2c\rho\sigma_{rad,w})} \tag{23c}$$

$$\frac{\partial^2 \tau_w}{\partial n_w^2} = 0 \tag{23d}$$

$$\frac{\partial \tau_w}{\partial \rho_s} = -\frac{8\pi c^4 n_w \rho^2 \sigma_{rad,w}^2}{A\omega^2 \rho_s^2(\eta_w \omega \rho_s + 2c\rho\sigma_{rad,w})} - \frac{8\pi c^4 \eta_w n_w \rho^2 \sigma_{rad,w}^2}{A\omega \rho_s(\eta_w \omega \rho_s + 2c\rho\sigma_{rad,w})^2} \tag{23e}$$

$$\frac{\partial^2 \tau_w}{\partial \rho_s^2} = \frac{16\pi c^4 \eta_w^2 n_w \rho^2 \sigma_{rad,w}^2}{A\rho_s(\eta_w \omega \rho_s + 2c\rho\sigma_{rad,w})^3} + \frac{16\pi c^4 n_w \rho^2 \sigma_{rad,w}^2}{A\omega^2 \rho_s^3(\eta_w \omega \rho_s + 2c\rho\sigma_{rad,w})} + \frac{16\pi c^4 \eta_w n_w \rho^2 \sigma_{rad,w}^2}{A\omega \rho_s^2(\eta_w \omega \rho_s + 2c\rho\sigma_{rad,w})^2} \tag{23f}$$

All the necessary quantities have by now been computed from the considerations introduced above and the resonant acoustic transmission sensitivity can thus be evaluated in Eq.22. Given that $\rho_s = \sum_{l=l_1}^{l_{max}} \rho_{m,l} h_l$ with $\rho_{m,l}$ the mass density of layer $l$ and $h_l$ its thickness, it is straightforward to derive the quantities $\frac{\partial \rho_s}{\partial \beta_i}\frac{\partial \rho_s}{\partial \beta_j}$ and $\frac{\partial^2 \rho_s}{\partial \beta_i \partial \beta_j}$ for the composite panel.

## 4 THE OPTIMISATION PROBLEM

The Newton's method will be hereby employed (ensuring quadratic convergence towards the solution) in order to optimise the considered set of parameters, which in the general orthotropic multilayer case can be expressed as

$$\mathbf{p} = \left\{ \; E_{x,1} E_{y,1} E_{z,1} v_{xy,1} v_{xz,1} v_{yz,1} G_{xy,1} G_{xz,1} G_{yz,1} h_1 \rho_{m,1} \cdots \rho_{m,l_{max}} \; \right\}^{\top} \tag{24}$$

with $l_{max}$ the maximum number of layers. It is interesting to note that including $\eta$ in an optimisation procedure will not provide any helpful information, as $\delta\eta$ will not directly affect neither the mass, nor the stiffness of the panel. On the other hand it will always be beneficial for the reduction of $\tau_w$, which suggests that a maximum $\eta$ will always be the result of the optimisation process. Some of the parameters may be considered to be constrained (e.g. $\beta_i \in [\beta_{i,min}, \beta_{i,max}]$). The objective function $\mathcal{F}(\mathbf{p})$ to be minimised is eventually to be decided. It is evident that the cost of added mass, as well as the one of static stiffness loss should be included in $\mathcal{F}(\mathbf{p})$ (if not maximising the mass of the panel would be the evident solution for minimising the acoustic transmission). There is a number of cost criteria that can be applied to the stress-strain matrix coefficients [37] of a laminate in order to account for its axial, shear and flexural stiffness. Dependence between the mass, stiffness and damping coefficient of each employed material can also be introduced.

The cost function can eventually be expressed as

$$\mathcal{F}(\mathbf{p}) = \xi_3\tau^3(\mathbf{p})+\xi_2\tau^2(\mathbf{p})+\xi_1\tau(\mathbf{p})+\xi_0+\delta_3\rho_s^3(\mathbf{p})+\delta_2\rho_s^2(\mathbf{p})+\delta_1\rho_s(\mathbf{p})+\delta_0+\zeta_3 d_s^3(\mathbf{p})+\zeta_2 d_s^2(\mathbf{p})+\zeta_1 d_s(\mathbf{p})+\zeta_0 \quad (25)$$

with $\xi_i$, $\delta_i$, $\zeta_i$ coefficients that allow the designer to apply a simple polynomial curve fitting to the available cost data, thus facilitating the differentiability of $\mathcal{F}(\mathbf{p})$. Higher order polynomial or exponential fitting functions may be applied without loss of accuracy.

## 5 NUMERICAL CASE STUDIES

In order to validate the exhibited optimisation approach, an asymmetric sandwich panel comprising two facesheets and a core is modelled in this section. The lower facesheet has a thickness $h_1$=1mm and is made of a material having $\rho_{m,1}$=3000e$^{-9}$kg/mm$^3$, $E_1 = 70$GPa and a Poisson's ration $v_1$=0.1. The upper facesheet has a thickness equal to $h_3$=2mm and is made of the same material as the lower facesheet. The core has a thickness $h_2$=10mm and is made of a material with $\rho_{m,2}$=50e$^{-9}$kg/mm$^3$, $E_2 = 0.07$GPa and $v_2$=0.4. Three FEs are used in the sense of thickness in order to model the structure. All computations were conducted using the R2013a version of MATLAB®.

### 5.1 Results on the wave sensitivity analysis of a layered structure

In this section the sensitivity of the wave characteristics with respect to the mechanical and geometric characteristics of the sandwich panel are sought as discussed in Sec.2. The results are compared to a FD approach throughout this section. In order to implement the FD approach a perturbation of 0.1% was considered for each structural parameter. The resulting FD sensitivity can be computed by

$$\frac{\partial k}{\partial \beta} = \frac{k_p - k_0}{\beta_p - \beta_0} \quad (26)$$

with $k_p$ the perturbed wavenumber value for $\beta_p$ and $\omega_0$ the corresponding wavenumber for the unperturbed parameter $\beta_0$.

The sensitivity of $k$ with respect to the thickness of the sandwich core layer is presented in Fig.3. A very interesting effect is that the influence of $\delta h_2$ on the flexural wavenumber becomes maximum for a certain frequency (approximately 2000 Hz), where the stiffening effect of $\delta h_2$ becomes maximum. An intense nonlinearity is observed in the relation of $\delta\omega$ to $\delta k$. A constant decrease of this influence is observed beyond that point. The stiffening effect is probably due to the greater separation of the two facesheets with $\delta h_2$. It is very probable however that for higher wavenumber values $\delta h_c$ will have a softening effect on the flexural wavenumber with the depicted curve passing to positive values ok $\delta k$.

In Fig.4, the sensitivity of $k$ with respect to the mass density of the sandwich facesheet layers is presented. As expected, both $\delta\rho_{m,1}$ and $\delta\rho_{m,3}$ will shift the wavenumber curve to higher values, suggesting a softening phenomenon. This effect will be greater for the thicker upper facesheet at low $k$ values. A highly nonlinear behaviour is again observed and it is interesting to see that there is a critical frequency value at which the effect of $\delta\rho_{m,1}$ and $\delta\rho_{m,3}$ will be the same. Beyond this critical wavenumber the softening effect will paradoxically be more intense for $\delta\rho_{m,1}$.

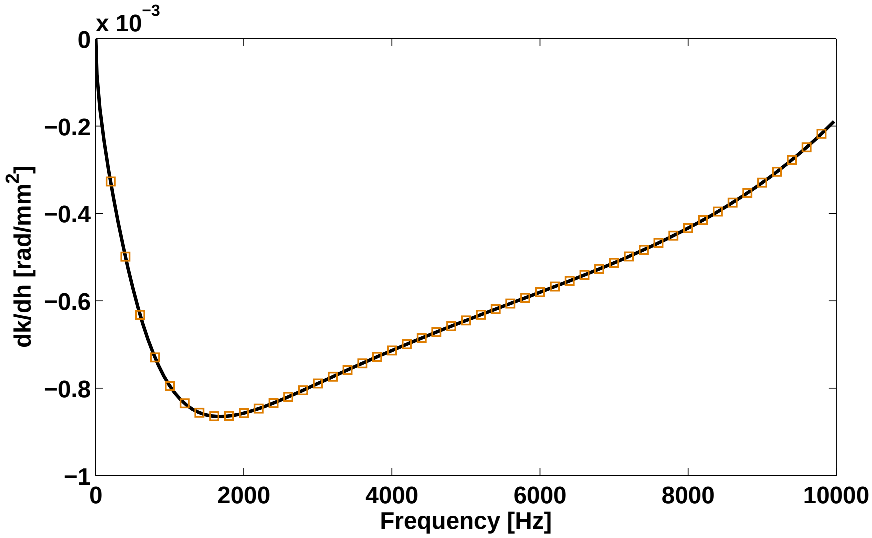


Figure 3: Sensitivity of the propagating wavenumber $k$ under a perturbation of $h_2$ for the first flexural wave type of the layered structure: Presented approach $(-)$, FD computation $(\square)$

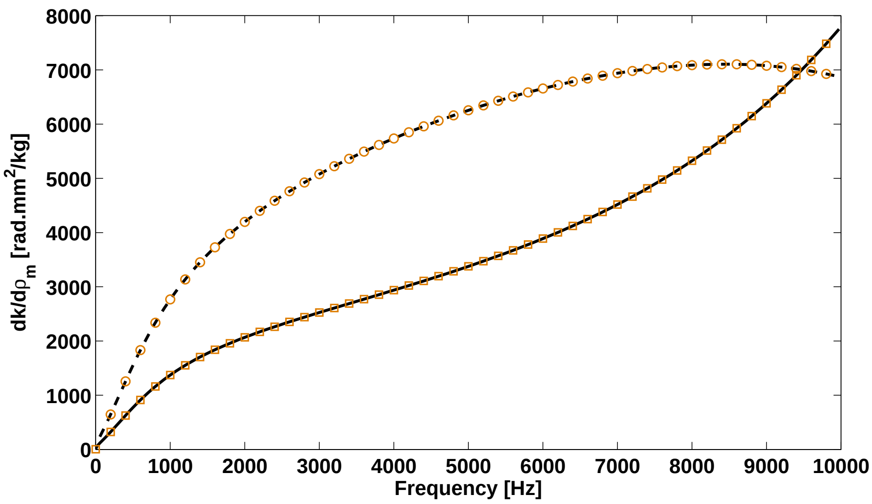


Figure 4: Sensitivity of the propagating wavenumber $k$ under a perturbation of the mass density of the sandwich facesheets for the first flexural wave type: Presented approach for $\rho_{m,1}$ $(-)$, FD computation for $\rho_{m,1}$ $(\square)$, Presented approach for $\rho_{m,3}$ $(--)$, FD computation for $\rho_{m,3}$ $(\circ)$

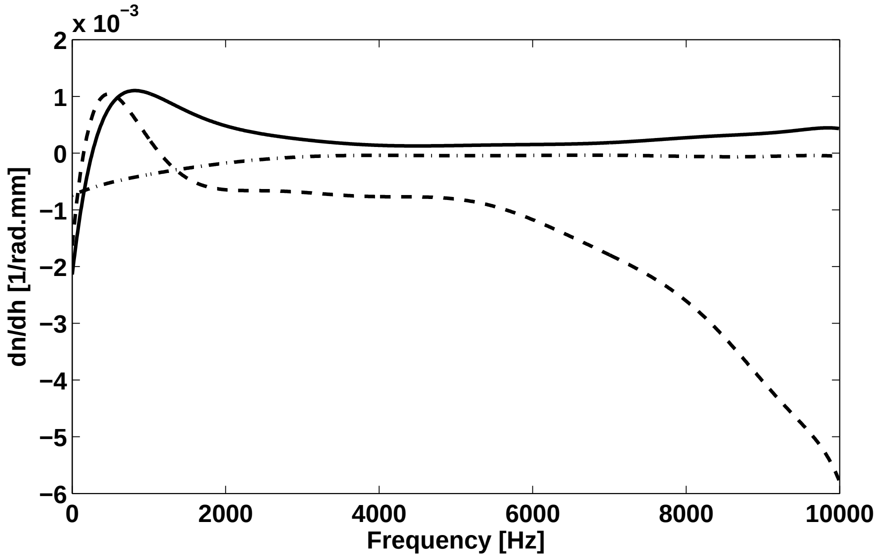


Figure 5: Sensitivity of the modal density $n$ of the first flexural propagating wave with respect to the layer thicknesses: with respect to the thickness of the lower facesheet $h_1$ (−), with respect to the thickness of the upper facesheet $h_3$ (−−), with respect to the thickness of the core $h_2$ ($- \cdot -$)

### 5.2 Results on the SEA sensitivity analysis of a layered structure

In this section the sensitivity of the SEA quantities, namely the modal density, the radiation efficiency and the damping loss factor are computed as discussed in Sec.3 and evaluated.

The first order sensitivity of the modal density of the composite panel with regard to the layer thicknesses are exhibited in Figs.5. It can be observed that the stiffening effect induced by $\delta h_3$ in the high frequency range, also induces a high reduction of the modal density, while a maximum softening effect is observed for both $\delta h_1$, $\delta h_3$ in the low frequency range (approximately 1000 Hz).

The sensitivity of the acoustic radiation efficiency for the composite panel with regard to the layer thicknesses is presented in Fig.6. In order to use a clearer logarithmic scale the quantity $\delta 10\log(\sigma)/\delta h$ is plotted. It is generally observed that altering the thickness of the thicker facesheet $h_3$ will have a maximum effect on the radiation efficiency, while the opposite is true for altering the thickness of the core layer. The maximum impact on $\sigma$ is as expected observed around the acoustic coincidence frequency (approximately 5800 Hz in this case study). It is interesting to note that the effect of $\delta h_1$ will have an opposite effect on $\sigma$ compared to $\delta h_3$.

The impact of the structural parameters on the acoustic transmission coefficient and the sound TL of the composite structure is eventually computed. In Fig.7 the sensitivity of the structure's TL with regard to the layer thicknesses is presented. It is evident that altering the thickness of the upper thicker layer will induce the maximum effect on TL, especially close to the acoustic coincidence region. On the other hand, altering the core thickness will have an insignificant effect on the TL index.

### 5.3 Structural design optimisation of the layered structure

As discussed in Sec.4, the criteria to be considered within the optimisation process of the mechanical and geometric characteristics of the panel are its mass, stiffness and vibroacoustic performance. The surface mass of the panel $\rho_s$ is chosen as a representative mass index, the total acoustic transmission coefficient $\tau$ is selected as the vibroacoustic performance index,

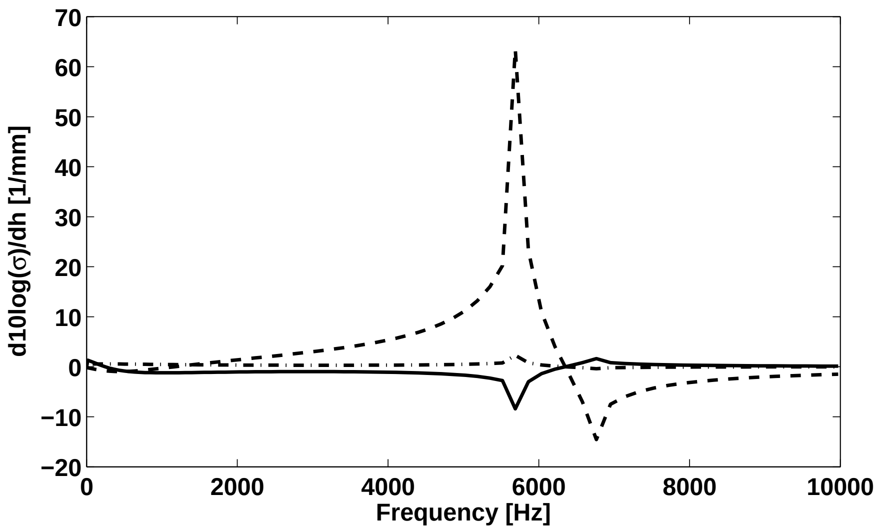


Figure 6: Sensitivity of the logarithmic acoustic radiation efficiency ($10\log(\sigma)$) of the first flexural propagating wave with respect to the layer thicknesses: with respect to the thickness of the lower facesheet $h_1$ ($-$), with respect to the thickness of the upper facesheet $h_3$ ($--$), with respect to the thickness of the core $h_2$ ($-\cdot-$)

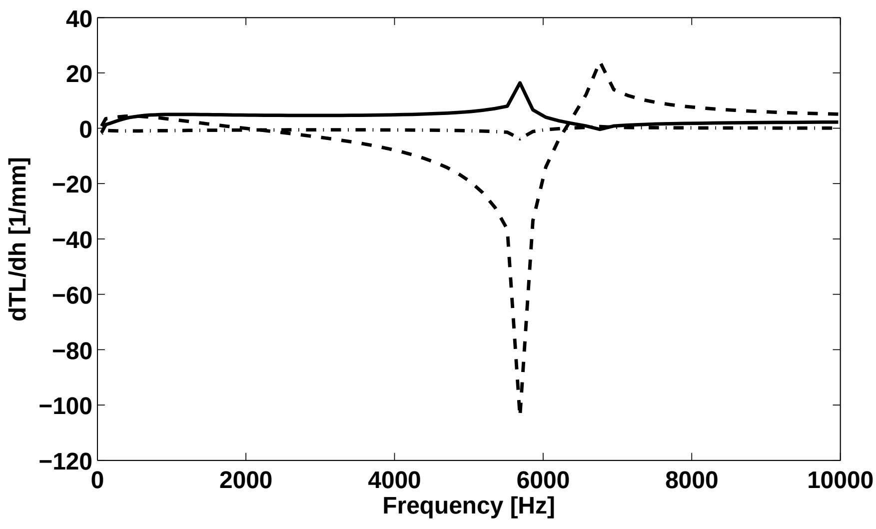


Figure 7: Sensitivity of the sound TL with respect to the layer thicknesses: with respect to the thickness of the lower facesheet $h_1$ ($-$), with respect to the thickness of the upper facesheet $h_3$ ($--$), with respect to the thickness of the core $h_2$ ($-\cdot-$)

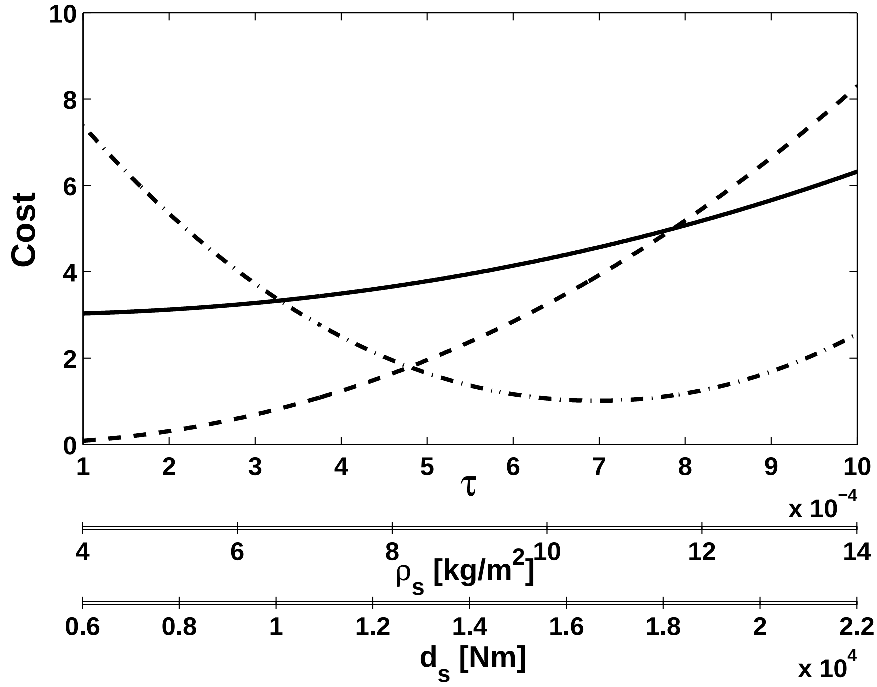


Figure 8: Representation of the cost functions employed within the current optimisation process. Cost function corresponding to: The acoustic transmission coefficient $\tau$ ($-$), The surface mass density $\rho_s$ ($--$), The flexural stiffness $d_s$ of the panel ($- \cdot -$)

while with regard to the structural stiffness and for the sake of simplicity we will hereby assume that we are solely interested in the sum of the static flexural stiffnesses of the panel $D_{xx}$, $D_{yy}$ expressed as

$$d_s = D_{xx} + D_{yy} = \frac{1}{3} \sum_{l=l_1}^{l_{max}} \left( (Q_{xx,l} + Q_{yy,l})(z_l^3 - z_{l-1}^3) \right) \tag{27a}$$

$$Q_{xx,l} = E_{x,l} \frac{1 - v_{yz,l}^2}{\Delta_l} \tag{27b}$$

$$Q_{yy,l} = E_{y,l} \frac{1 - v_{xz,l}^2}{\Delta_l} \tag{27c}$$

$$\Delta_l = 1 - v_{xy,l}^2 - v_{yz,l}^2 - v_{zx,l}^2 - 2 v_{xy,l} v_{yz,l} v_{zx,l} \tag{27d}$$

which in the case of an isotropic composite panel gives

$$d_s = \frac{2}{3} \sum_{l=l_1}^{l_{max}} \left( Q_l (z_l^3 - z_{l-1}^3) \right) \tag{28}$$

with $z_l$ the coordinate of the upper surface of layer $l$ in the thickness direction. The design cost functions, employed in order to decide the relation between $\rho_s$, $\tau$ and $d_s$ and the corresponding induced design cost are exhibited in Fig.8.

Additional constraints (e.g. minimum axial and/or flexural stiffness, maximum surface mass e.t.c) can be considered. The constrained optimization problem is solved using Newton's method.

### 5.4 Optimal parameters and discussion on the computational efficiency

The optimisation problem is solved for $k = 0.13$rad/mm, and the optimal material and geometric parameters that minimise the sum of the costs as presented in Fig.8 are computed as follows

$$E_1 = 80.9\text{GPa},\ v_1 = 0.12,\ h_1 = 1.19\text{mm},\ \rho_{m,1} = 1647\text{kg/m}^3$$
$$E_2 = 110\text{MPa},\ v_2 = 0.37,\ h_2 = 10.53\text{mm},\ \rho_{m,2} = 14.6\text{kg/m}^3$$
$$E_3 = 58.3\text{GPa},\ v_3 = 0.19,\ h_3 = 1.74\text{mm},\ \rho_{m,3} = 1500\text{kg/m}^3$$

It is noted that the only quantities laying on the limits of the predefined constraints which could potentially further improve the overall structural performance are the Young's modulus of the core layer $E_2$ as well as the mass density of the upper layer $\rho_{m,3}$. Optimising the structure in a broadband frequency range can be done by averaging the optimal parameters over the frequency range of interest or by introducing a weighting average for the frequency bands that are considered more important (e.g. frequency of the external acoustic excitation). The optimisation process was completed in 8 iterations each of which lasted approximately 78 seconds, resulting in a total computation time of 630s. This suggests that a broadband structural optimisation is feasible within a few hours, even with a conventional computing equipment.

## 6 Conclusions

In this work, the optimal mechanical and geometric characteristics for layered composite structures subject to vibroacoustic excitations were derived in a wave SEA context. The main conclusions of the paper are summarised as:

(i) An intense frequency dependent variation of the sensitivity of the propagating wave characteristics has been observed as a function of the design of the composite structure. This also implies frequency dependence of the optimal design parameters.

(ii) Expressions for the first and second order sensitivities of the SEA quantities, namely the modal density and the radiation efficiency of the composite panel were derived. The design parametric sensitivity for each of the SEA quantities, as well as of the acoustic transmission coefficient were found to be highly frequency dependent. The impact of the design alteration on the vibroacoustic response was maximised in the vicinity of the acoustic coincidence range for most parameters.

(iii) The suggested optimisation process is computationally efficient, allowing for a broadband structural optimisation of a layered structure in a rational period of time, even with the use of a conventional computing equipment.

## REFERENCES

[1] D. J. Mead, "A general theory of harmonic wave propagation in linear periodic systems with multiple coupling," *Journal of Sound and Vibration*, vol. 27, no. 2, pp. 235–260, 1973.

[2] R. Langley, "A note on the force boundary conditions for two-dimensional periodic structures with corner freedoms," *Journal of Sound and Vibration*, vol. 167, no. 2, pp. 377–381, 1993.

[3] V. Cotoni, R. S. Langley, and P. J. Shorter, “A statistical energy analysis subsystem formulation using finite element and periodic structure theory,” *Journal of Sound and Vibration*, vol. 318, no. 4-5, pp. 1077–1108, 2008.

[4] B. R. Mace, D. Duhamel, M. J. Brennan, and L. Hinke, “Finite element prediction of wave motion in structural waveguides,” *The Journal of the Acoustical Society of America*, vol. 117, no. 5, pp. 2835–2843, 2005.

[5] J.-M. Mencik and M. Ichchou, “Multi-mode propagation and diffusion in structures through finite elements,” *European Journal of Mechanics-A/Solids*, vol. 24, no. 5, pp. 877–898, 2005.

[6] G. Maidanik, “Response of ribbed panels to reverberant acoustic fields,” *the Journal of the Acoustical Society of America*, vol. 34, no. 6, pp. 809–826, 1962.

[7] C. Wallace, “Radiation resistance of a rectangular panel,” *The Journal of the Acoustical Society of America*, vol. 51, no. 3B, pp. 946–952, 1972.

[8] R. Lyon, *Statistical energy analysis of dynamical systems: theory and applications*. MIT press Cambridge, 1975.

[9] F. G. Leppington, E. G. Broadbent, and K. H. Heron, “Acoustic radiation efficiency of rectangular panels,” in *Proceedings of The Royal Society of London, Series A: Mathematical and Physical Sciences*, vol. 382, pp. 245–271, 1982.

[10] S. Ghinet, N. Atalla, and H. Osman, “The transmission loss of curved laminates and sandwich composite panels,” *The Journal of the Acoustical Society of America*, vol. 118, no. 2, pp. 774–790, 2005.

[11] D. Chronopoulos, M. Ichchou, B. Troclet, and O. Bareille, “Computing the broadband vibroacoustic response of arbitrarily thick layered panels by a wave finite element approach,” *Applied Acoustics*, vol. 77, pp. 89–98, 2014.

[12] D. Chronopoulos, B. Troclet, M. Ichchou, and J. Lainé, “A unified approach for the broadband vibroacoustic response of composite shells,” *Composites Part B: Engineering*, vol. 43, no. 4, pp. 1837–1846, 2012.

[13] D. Chronopoulos, B. Troclet, O. Bareille, and M. Ichchou, “Modeling the response of composite panels by a dynamic stiffness approach,” *Composite Structures*, vol. 96, pp. 111–120, 2013.

[14] D. Chronopoulos, M. Ichchou, B. Troclet, and O. Bareille, “Efficient prediction of the response of layered shells by a dynamic stiffness approach,” *Composite Structures*, vol. 97, pp. 401–404, 2013.

[15] D. Chronopoulos, M. Ichchou, B. Troclet, and O. Bareille, “Predicting the broadband vibroacoustic response of systems subject to aeroacoustic loads by a krylov subspace reduction,” *Applied Acoustics*, vol. 74, no. 12, pp. 1394–1405, 2013.

[16] D. Chronopoulos, M. Ichchou, B. Troclet, and O. Bareille, “Thermal effects on the sound transmission through aerospace composite structures,” *Aerospace Science and Technology*, vol. 30, no. 1, pp. 192–199, 2013.

[17] D. Chronopoulos, M. Ichchou, B. Troclet, and O. Bareille, "Predicting the broadband response of a layered cone-cylinder-cone shell," *Composite Structures*, vol. 107, pp. 149–159, 2014.

[18] R. B. Nelson, "Simplified calculation of eigenvector derivatives," *AIAA journal*, vol. 14, no. 9, pp. 1201–1205, 1976.

[19] R. T. Haftka and H. M. Adelman, "Recent developments in structural sensitivity analysis," *Structural optimization*, vol. 1, no. 3, pp. 137–151, 1989.

[20] S. Adhikari and M. I. Friswell, "Eigenderivative analysis of asymmetric non-conservative systems," *International Journal for Numerical Methods in Engineering*, vol. 51, no. 6, pp. 709–733, 2001.

[21] K. K. Choi and N.-H. Kim, *Structural sensitivity analysis and optimization 1: linear systems*, vol. 1. Springer, 2006.

[22] K. Sobczyk, *Stochastic wave propagation*. Elsevier, 1985.

[23] A. Belyaev, "Comparative study of various approaches to stochastic elastic wave propagation," *Acta mechanica*, vol. 125, no. 1-4, pp. 3–16, 1997.

[24] K. Koo, B. Pluymers, W. Desmet, and S. Wang, "Vibro-acoustic design sensitivity analysis using the wave-based method," *Journal of Sound and Vibration*, vol. 330, no. 17, pp. 4340–4351, 2011.

[25] M. Ruzzene and F. Scarpa, "Directional and band-gap behavior of periodic auxetic lattices," *physica status solidi (b)*, vol. 242, no. 3, pp. 665–680, 2005.

[26] M. Ichchou, F. Bouchoucha, M. Ben Souf, O. Dessombz, and M. Haddar, "Stochastic wave finite element for random periodic media through first-order perturbation," *Computer Methods in Applied Mechanics and Engineering*, vol. 200, no. 41, pp. 2805–2813, 2011.

[27] B. Souf, O. Bareille, M. Ichchou, F. Bouchoucha, and M. Haddar, "Waves and energy in random elastic guided media through the stochastic wave finite element method," *Physics Letters A*, vol. 377, no. 37, pp. 2255–2264, 2013.

[28] R. Le Riche and R. T. Haftka, "Optimization of laminate stacking sequence for buckling load maximization by genetic algorithm," *AIAA journal*, vol. 31, no. 5, pp. 951–956, 1993.

[29] M. Walker and R. E. Smith, "A technique for the multiobjective optimisation of laminated composite structures using genetic algorithms and finite element analysis," *Composite Structures*, vol. 62, no. 1, pp. 123–128, 2003.

[30] S. Omkar, D. Mudigere, G. N. Naik, and S. Gopalakrishnan, "Vector evaluated particle swarm optimization (vepso) for multi-objective design optimization of composite structures," *Computers & structures*, vol. 86, no. 1, pp. 1–14, 2008.

[31] R. Langley, N. Bardell, and P. Loasby, "The optimal design of near-periodic structures to minimize vibration transmission and stress levels," *Journal of Sound and Vibration*, vol. 207, no. 5, pp. 627–646, 1997.

[32] M. I. Hussein, G. M. Hulbert, and R. A. Scott, “Dispersive elastodynamics of 1d banded materials and structures: analysis,” *Journal of sound and vibration*, vol. 289, no. 4, pp. 779–806, 2006.

[33] M. I. Hussein, K. Hamza, G. M. Hulbert, R. A. Scott, and K. Saitou, “Multiobjective evolutionary optimization of periodic layered materials for desired wave dispersion characteristics,” *Structural and Multidisciplinary Optimization*, vol. 31, no. 1, pp. 60–75, 2006.

[34] M. Collet, K. A. Cunefare, and M. N. Ichchou, “Wave motion optimization in periodically distributed shunted piezocomposite beam structures,” *Journal of Intelligent Material Systems and Structures*, 2008.

[35] J. Allard and N. Atalla, *Propagation of Sound in Porous Media: Modelling Sound Absorbing Materials 2e*. John Wiley & Sons, 2009.

[36] R. Courant and D. Hilbert, *Methoden der mathematischen Physik*, *vol. 1*, vol. 2. Berlin, 1931.

[37] R. M. Jones, *Mechanics of composite materials*. CRC Press, 1998.